Solid-State Electronics 53 (2009) 102–106

Contents lists available at ScienceDirect

Solid-State Electronics

journal homepage: www.elsevier.com/locate/sse

Metamorphic $In_{0.7}Al_{0.3}As/In_{0.69}Ga_{0.31}As$ thermophotovoltaic devices grown on graded $InAs_yP_{1-y}$ buffers by molecular beam epitaxy

Mantu K. Hudait *, M. Brenner, S.A. Ringel [1]

Department of Electrical and Computer Engineering, The Ohio State University, Columbus, OH 43210, United States

ARTICLE INFO

Article history:
Received 20 May 2008
Received in revised form 9 October 2008
Accepted 20 October 2008
Available online 3 December 2008

The review of this paper was arranged by Prof. E. Calleja

Keywords:
InGaAs
TPV
MBE
Lattice-mismatch
InAsP
InAlAs
Window layer

ABSTRACT

The application of an $In_{0.7}Al_{0.3}As$ window layer material on the properties of lattice-mismatched (LMM) single-junction (SJ) $In_{0.69}Ga_{0.31}As$ thermophotovoltaic (TPV) cells grown by solid source molecular beam epitaxy (MBE) was studied as an alternative to conventional InAsP window layers. For these 0.60 eV bandgap SJ devices, high performance was achieved, displaying open-circuit voltage of 355 mV, power density of 0.532 W/cm^2 and a fill factor of 66.5% measured at a current density value of 2.26 A/cm^2. The measured internal quantum efficiencies were close to ~100% at wavelengths between approximately 1.2–1.4 mm, suggestive that low carrier recombination rates in the vicinity of this alternative $In_{0.70}Al_{0.30}As/In_{0.69}Ga_{0.31}As$ window/emitter interface has been achieved. The quantum efficiency data coupled with the device parameters show that InAlAs can be successfully substituted for conventional InAsP window layers in metamorphic TPV devices. By using an interface consisting solely of III-As alloys for the window/emitter material pairing as opposed to the conventional InAsP/InGaAs window/emitter design, this approach avoids the problematic III-P/III-As interface transition for MBE growth of TPV devices that has been shown to impact carrier collection efficiency [Hudait MK, Lin Y, Palmisiano MN, Ringel SA. 0.6-eV band gap $In_{0.69}Ga_{0.31}As$ thermophotovoltaic devices grown on $InAs_yP_{1-y}$ step-graded buffers by molecular beam epitaxy. IEEE Electron Dev Lett 2003;24(9):538–40].

1. Introduction

$In_xGa_{1-x}As$ based thermophotovoltaic (TPV) devices grown on InP substrates are of interest for a variety of terrestrial and space energy conversion applications [1–7]. For high conversion efficiency and power density, InGaAs TPV cells with band gaps from 0.50 eV to 0.74 eV are required. To achieve these band gaps requires an In content (x) of the active $In_xGa_{1-x}As$ TPV layers well in excess of the 53% composition that provides a convenient lattice match to InP substrates. The subsequent lattice mismatch between the $In_xGa_{1-x}As$ TPV device and the InP substrate (1.1% for 0.6 eV bandgap TPV cells) necessitates a buffer scheme to reduce the threading dislocation density that would otherwise propagate through the device layers. Also, the emitter bulk material and interface quality between the internally lattice-matched emitter and window layers are of great importance for achieving high-performance TPV cells, as these regions impact minority carrier collection efficiency [8,9], in particular at shorter wavelengths.

TPV cells based on $In_xGa_{1-x}As$ can utilize one of several window layer materials. InAsP is commonly adopted to provide a classic, symmetrical InAsP/InGaAs/InAsP double heterostructure design since InAsP is also used for both the back surface field and graded buffer layers in common metal–organic chemical vapor deposition (MOCVD) grown TPV cells [5–7,10]. However, solid source molecular beam epitaxy (MBE) is now receiving interest for TPV applications due to its extreme precision and growth uniformity [2], and since it provides an opportunity to investigate and potentially optimize lattice-mismatched (LMM) TPV structures within a very different growth regime compared to MOCVD. On the other hand, for TPV structures grown using MBE, the use of InAsP windows on InGaAs TPV devices is complicated by the need for a short growth interruption at the InAsP/InGaAs window/emitter interface. This is required to establish optimum arsenic and phosphorus beam fluxes prior to growth of the thin $InAs_yP_{1-y}$ window layer that must be lattice matched to the $In_xGa_{1-x}As$ emitter. We have demonstrated the sensitivity of local carrier recombination to the interface switching conditions for InP/InGaAs interfaces [11]. Typical 0.6 eV bandgap InGaAs TPV cells require an $InAs_{0.32}P_{0.68}$ composition window layer to maintain lattice matching, resulting in a nominal bandgap of ~1 eV for the passive window layer [12,13]. In contrast, the $In_xAl_{1-x}As$ material system, which has been relatively unexplored for TPV applications, also provides lattice-matched window choices for $In_xGa_{1-x}As$ TPV devices, and for the

* Corresponding author. Present address: Components Research, Intel Corporation, Hillsboro, OR 97124, United States. Tel.: +1 503 613 2199; fax: +1 971 214 7807.
E-mail addresses: mantu.k.hudait@intel.com (M.K. Hudait), ringel@ece.osu.edu (S.A. Ringel).
[1] Tel.: +1 614 292 6904; fax: +1 614 292 9562.

0038-1101/$ - see front matter © 2008 Elsevier Ltd. All rights reserved.
doi:10.1016/j.sse.2008.10.007

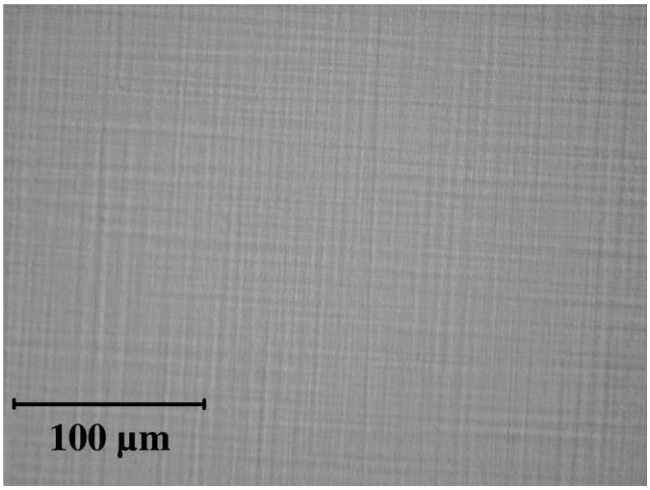

Fig. 1. Nomarski image of an $In_{0.69}Ga_{0.31}As$ TPV device structure grown on InP substrate using $InAs_yP_{1-y}$ step-graded buffer.

same 0.6 eV InGaAs bandgap cell, a lattice-matched $In_{0.7}Al_{0.3}As$ would also provide a nominal window layer bandgap of ~1 eV [12]. From the perspective of MBE growth, an InAlAs/InGaAs window/emitter structure within a TPV cell would avoid the need for a growth interruption at the crucial window/emitter interface, which may improve the short wavelength performance reported for earlier MBE-grown TPV devices [2].

In this study, the effect of using an $In_{0.7}Al_{0.3}As$ window layer on the properties of lattice-mismatched (LMM) single-junction (SJ) n/p $In_{0.69}Ga_{0.31}As$ TPV cell has been investigated. The LMM $In_{0.69}Ga_{0.31}As$ TPV device structures grown by MBE were analyzed by cross-sectional transmission electron microscopy (XTEM), triple crystal X-ray diffraction and Nomarski microscopy to evaluate defect properties, strain relaxation and surface morphology, respectively. Single junction LMM $In_{0.69}Ga_{0.31}As$ TPV devices with band gaps of 0.6 eV were processed and high performance is achieved for these cells implies $In_{0.7}Al_{0.3}As$ layer can be used as an alternative window layer material for $In_{0.69}Ga_{0.31}As$ TPV device structures.

2. MBE growth and device processing

Lattice-mismatched SJ $In_{0.69}Ga_{0.31}As$ TPV structures were grown on semi-insulating 2° offcut (100) InP substrates using a solid source MBE system equipped with valved cracker sources for arsenic and phosphorus. InP substrate oxide desorption was performed at 510 °C under a phosphorus overpressure of $\sim 1 \times 10^{-5}$ Torr and verified by observing a strong (2×4) reflection high-energy electron diffraction (RHEED) pattern, indicating a clean (100) InP surface. An undoped 0.2 μm InP buffer layer was then deposited under a stabilized P_2 flux prior to the growth of an n-type Si-doped $InAs_yP_{1-y}$ step-graded buffer. The step-graded $InAs_yP_{1-y}$ buffer consisted of 4-steps, with the final compositions of $InAs_{0.32}P_{0.68}$ providing a lattice-matched "virtual" substrate for $In_{0.69}Ga_{0.31}As$ TPV overgrowth. The surface morphology of LMM $In_{0.69}Ga_{0.31}As$ TPV device grown on InP substrate using $InAs_yP_{1-y}$ step-graded buffer shown in Fig. 1 exhibits a well-developed 2D crosshatch pattern and this uniform crosshatch pattern is an indication of metamorphic device layer growth. Reciprocal space maps (RSMs) using triple crystal X-ray diffraction were used to determine the alloy composition, strain relaxation and the internally lattice-matched condition to the upper layer of $InAs_yP_{1-y}$ step-graded buffer $InAs_{0.32}P_{0.68}$, $In_{0.69}Ga_{0.31}As$ device layer and $In_{0.7}Al_{0.3}As$ window layer. Fig. 2a and b shows the RSMs for (004) and (115)

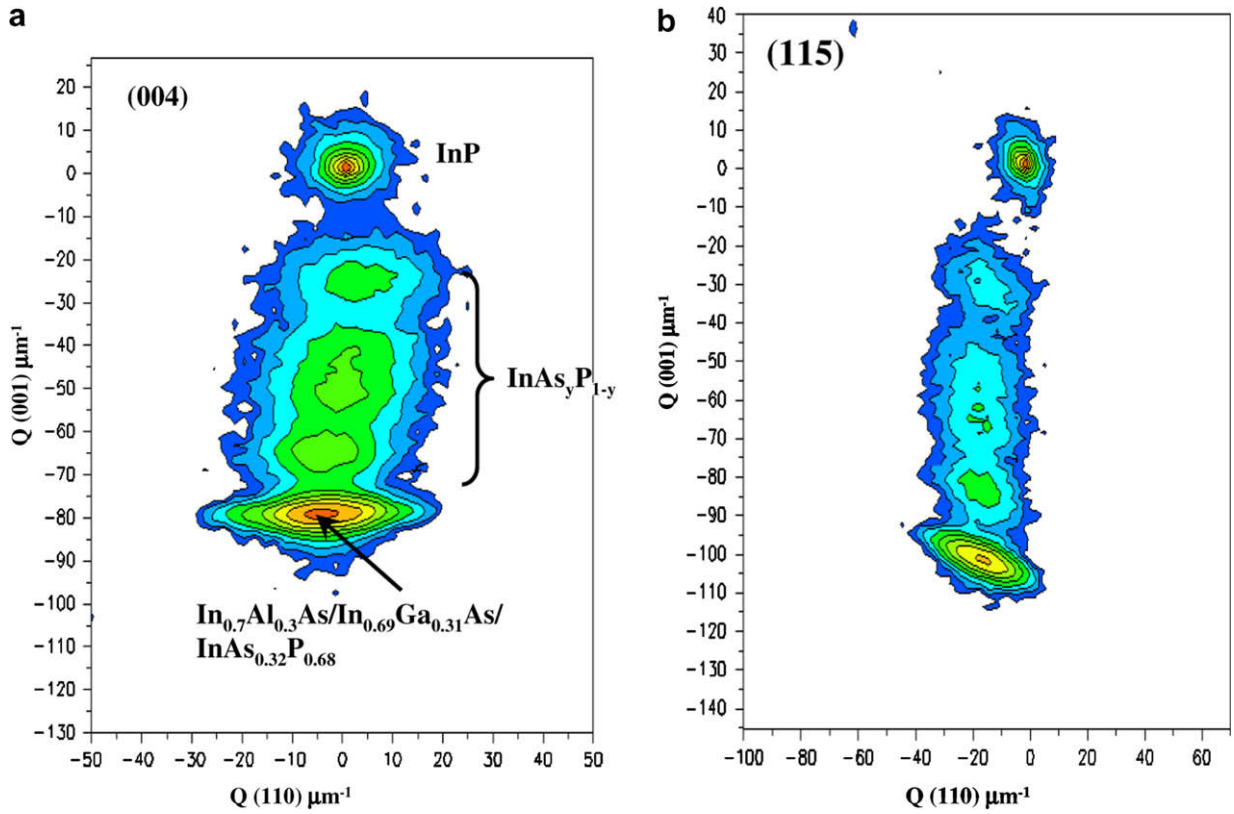

Fig. 2. (a) Symmetric (004) and (b) asymmetric (115) reciprocal space maps of an $In_{0.7}Al_{0.3}As/In_{0.69}Ga_{0.31}As/InAs_{0.32}P_{0.68}$ TPV device structure grown on (001) InP substrate using $InAs_yP_{1-y}$ step-graded buffer obtained using an incident X-ray beam oriented along the [110] direction.

reflections from LMM $In_{0.69}Ga_{0.31}As$ TPV device structure grown on InP substrate with the incident beam is along the [1 1 0] direction. In Fig. 2a, the (0 0 4) reciprocal space maps exhibit five distinct reciprocal lattice units (RLP) which corresponds to the InP substrate, three steps in $InAs_yP_{1-y}$ graded buffer and the lattice-matched $In_{0.69}Ga_{0.31}As$ layer. The $In_{0.7}Al_{0.3}As/In_{0.69}Ga_{0.31}As$ layer RLP lies directly on the $InAs_{0.32}P_{0.68}$ buffer layer, thus in-plane lattice constant of the $In_{0.69}Ga_{0.31}As$ layer is coherent with the uppermost buffer layer, indicating a close internally lattice-matched condition. The degree of relaxation of the $In_{0.69}Ga_{0.31}As$ overlayer is found to be more than 90% along with the measured values of in-plane lattice constant (from Fig. 2b) and out-of-plane lattice constant (from Fig. 2a). Full details on the growth and properties of the $InAs_yP_{1-y}$ step-graded buffer and the minority carrier

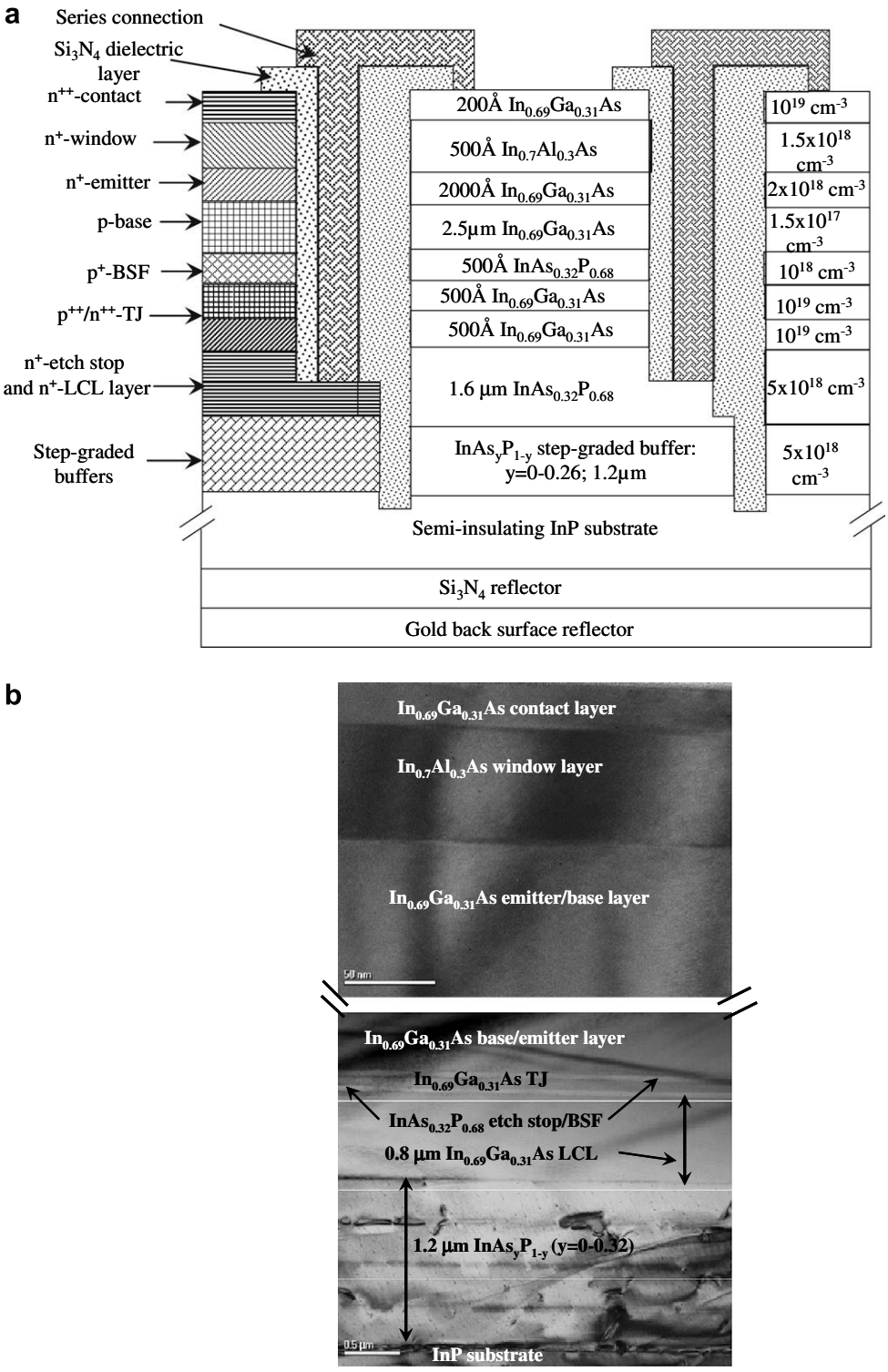

Fig. 3. (a) Schematic cross-section and (b) cross-sectional TEM micrograph of a typical lattice-mismatched $In_{0.69}Ga_{0.31}As$ n/p/n TPV test structure grown with an $In_{0.7}Al_{0.3}As$ window layer and $InAs_yP_{1-y}$ step-graded buffer on InP substrate.

lifetime of $In_{0.69}Ga_{0.31}As$ on top of this $InAs_yP_{1-y}$ step-graded buffer were previously reported [3,14,15].

The schematic cross-section of LMM n/p/n $In_{0.69}Ga_{0.31}As$ TPV structure shown in Fig. 3a with an $In_{0.7}Al_{0.3}As$ window layer allows the use of the desired n-on-p cell configuration with an n-type $InAs_{0.32}P_{0.68}$ lateral conduction layer (LCL) to interconnect strings of lateral devices in series to achieve a TPV monolithic interconnected module (MIM) [5–7,16,17]. Fig. 3b shows a cross-sectional TEM micrograph of a LMM $In_{0.69}Ga_{0.31}As$ TPV structure grown on an InP substrate with a metamorphic $InAs_yP_{1-y}$ buffer by MBE that is representative of our TPV growths regardless of which window layer material ($InAs_{0.32}P_{0.68}$ or $In_{0.7}Al_{0.3}As$) is used. The misfit and threading dislocations are predominantly contained in the buffer layer, and plan-view TEM measurements previously revealed threading dislocation densities on the order of $2–4 \times 10^6\ cm^{-2}$ within the active device layers [14]. The thickness and doping level in the n-type $In_{0.69}Ga_{0.31}As$ emitter were optimized by growing several n/p $In_{0.69}Ga_{0.31}As$ diode structures on $InAs_yP_{1-y}$/InP substrates. Ti/Au (200 Å/3 μm) metallization was used for both front and back ohmic contacts, and a silicon nitride (Si_3N_4) dielectric layer was deposited using plasma enhanced chemical vapor deposition to prevent the interconnect metallization from short-circuiting the individual cells in the MIM configuration. A similar Si_3N_4 layer was used on the top surface of the $In_{0.7}Al_{0.3}As$ window layer after removal of the heavily doped $In_{0.69}Ga_{0.31}As$ cap, to act as an anti-reflection coating (ARC). On the backside of the semi-insulating InP substrate, a Si_3N_4/Au coating was used as a back surface reflector to reflect the light not absorbed on the first pass and to recuperate sub-bandgap light at the radiator. A full description of the TPV device design and processing can be found in earlier papers [2,3].

3. Results and discussion

The electrical quality of the single-junction (SJ) TPV cells was evaluated using a quartz halogen lamp assembly to measure short-circuit current (I_{sc}), open-circuit voltage (V_{oc}), and fill factor (FF) to determine the maximum output power ($P_{max} = V_{oc} * I_{sc} * FF$). The light source is a quartz halogen tungsten lamp whose spectral emission fits a graybody spectrum with a temperature of 1920 K (emissivity = 0.0230) and 2050 K (emissivity = 0.0252) with the intensity at the cell being controlled (diminished) by reducing the solid angle of illumination viewed by the cell. Fig. 4a and b shows *J–V* characteristics obtained at 1920 K and 2050 K, respectively, from these single-junction TPV cells. Short-circuit current density (J_{sc}), open-circuit voltage (V_{oc}), fill factor (FF) and output power (P_{max}) values of 1.11 A/cm^2, 334 mV, 65.6% and 6.9 mW, respectively, were obtained for a SJ cell at 1920 K and J_{sc}, V_{oc}, FF and P_{max} values of 2.26 A/cm^2, 355 mV, 66.5% and 15 mW (0.532 W/cm^2), respectively, were obtained from the same cell measured at 2050 K. These V_{oc} values are comparable to those obtained from similar 0.6 eV bandgap TPV cells grown by MOCVD and MBE that employed more typical $InAs_{0.32}P_{0.68}$ window layer materials [2,5–7].

In order to investigate the dominant current transport mechanisms for this SJ TPV cell, a series of *J–V* measurements were performed by varying light intensities to measure J_{sc}, V_{oc}, and FF. Fig. 5 shows J_{sc} versus V_{oc} data obtained for a SJ TPV device, where an increase in J_{sc} corresponds to an increase in light intensity for the *J–V* measurements. The value of V_{oc} increases logarithmically with J_{sc}, as expected, and by performing a linear fit of the data in Fig. 5 and using the ideal diode equation [1]

$$J_{sc} = J_o\left\{\exp\left(\frac{qV_{oc}}{nkT_{cell}}\right) - 1\right\}, \quad (1)$$

where n, the diode ideality factor and J_o, the dark saturation current density, can be estimated [4]. In this expression, k is the Boltzmann

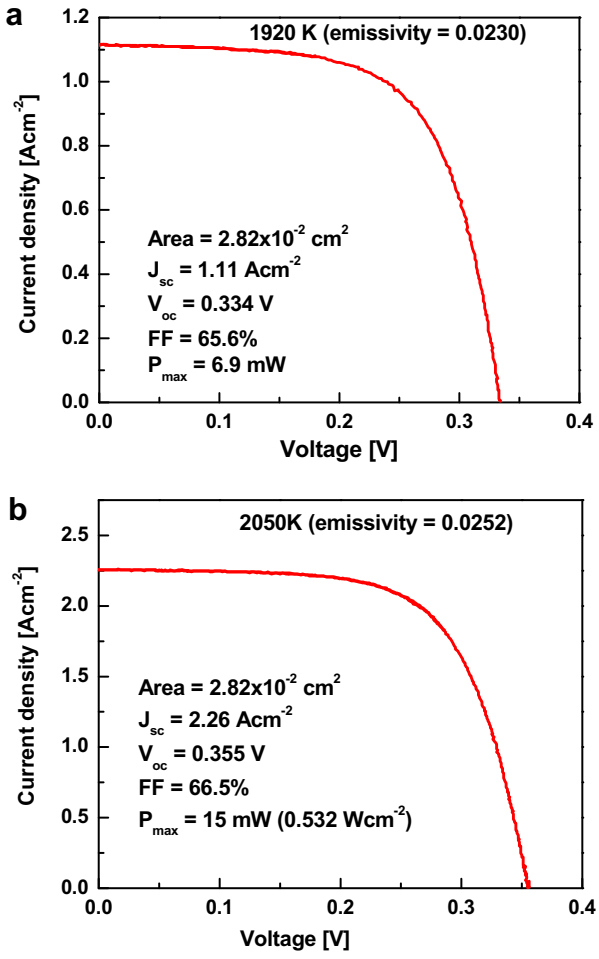

Fig. 4. Current density versus voltage characteristics of SJ $In_{0.69}Ga_{0.31}As$ TPV cell at (a) 1920 K and (b) 2050 K, respectively. The light source is a quartz halogen tungsten lamp whose spectral emission matches a graybody spectrum with a temperature of 1920 K (emissivity = 0.0230) and 2050 K (emissivity = 0.0252).

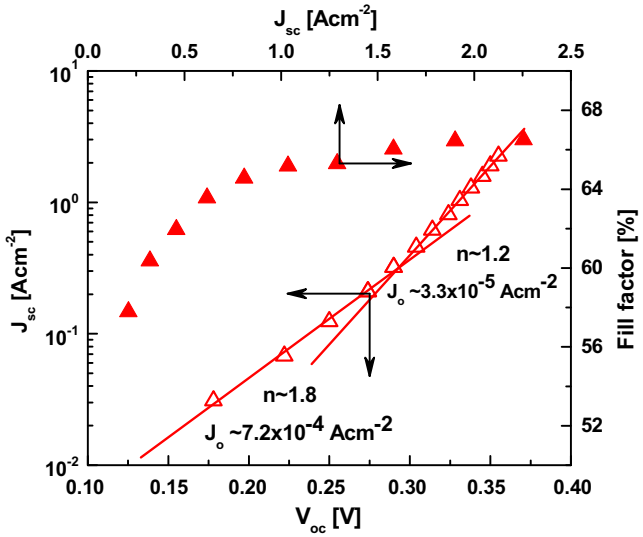

Fig. 5. Variation of short-circuit current density (J_{sc}) with open-circuit voltage (V_{oc}) and fill factor (FF) with J_{sc} for a SJ TPV cell with E_g = 0.60 eV obtained as a function of incident light intensity. The fill factor value approaches ~66% at higher illumination intensities.

constant and T_{Cell} is the temperature of the cell during measurement (kept constant at 298 K). The data implies a change in the dominant transport mechanism from one that is likely to be depletion region recombination-limited at lower light intensities (denoted by the $n \sim 1.8$ region in the figure) to one that is more controlled by injection/diffusion in the higher injection regime, which is where TPV devices typically operate. In this higher injection regime, a linear fit yields $n \approx 1.2$, with the extracted value for J_o determined to be 3.3×10^{-5} A/cm^2. The fill factor as a function of J_{sc} is also shown in Fig. 5 and approaches ~66% at higher illumination intensities. These performance values were observed with a high degree of uniformity (±1% of cell parameters J_{sc}, V_{oc}, FF and P_{max}) across a 2 in. InP wafer under identical illumination conditions and intensities (1920 K graybody spectrum; emissivity of 0.0230). This is particularly noteworthy for V_{oc} and FF, which are sensitive to the impact of small variations in material uniformity on device recombination and shunting. The high performance and uniformity of the devices implies very high quality growth of the InAlAs window and of the InAlAs/InGaAs window/emitter interface.

Internal quantum efficiency (IQE) measurements were used to further investigate the detailed carrier collection efficiency for the $In_{0.69}Ga_{0.31}As/In_{0.7}Al_{0.3}As$ emitter/window heterostructures and of the entire TPV cell structure. The IQE data were obtained using the measured external quantum efficiency and reflectance from the SJ TPV cell. As seen in Fig. 6, uniform and very high (~97%) quantum efficiencies are obtained from a SJ $In_{0.69}Ga_{0.31}As$ TPV cell for photon wavelengths in excess of ~1.4 μm. This illustrates the effectiveness of the $In_{0.69}Ga_{0.31}As$ n/p junction in collecting photo-generated minority carrier electron throughout the p-type base layer. It also indicates a high carrier lifetime and a diffusion length in excess of the 2.5 μm base thickness for minority carrier electrons in the p-type $In_{0.69}Ga_{0.31}As$ base layer. However, in the shorter wavelength region, which is more sensitive to recombination within the emitter/window interface, an even higher value of IQE is maintained for this SJ TPV cell, approaching ~100%. These results demonstrate the general viability of using InAlAs window layers as an alternative for InAsP within InGaAs-based TPV devices. More specifically for MBE growth, by substituting InAlAs/InGaAs/InAsP heterostructure design for the more conventional symmetric InAsP/InGaAs/InAsP heterostructure, known growth transition issues [2] at the window/emitter interface that are problematic due to switching from a non-P containing emitter layer (InGaAs) to a P-containing window layer (InAsP), the conventional double heterostructure design have been completely avoided.

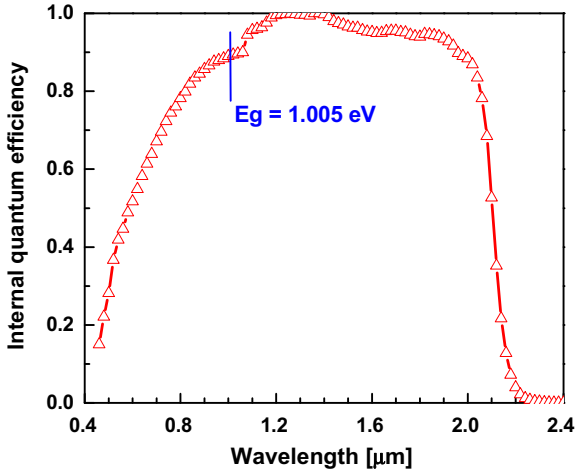

Fig. 6. Internal quantum efficiency of a SJ TPV cell with E_g = 0.60 eV. The band gap, 1.005 eV (Ref. [12]) of $In_{0.7}Al_{0.3}As$ window layer is indicated in this figure.

4. Conclusion

This paper describes the application of $In_{0.7}Al_{0.3}As$ window layer material on a lattice-mismatched $In_{0.69}Ga_{0.31}As$ TPV cells grown by MBE. High performance devices were obtained, with SJ cells displaying a V_{oc} of 0.355 V, FF of 66.5% and power density of 0.532 W/cm^2 measured at a J_{sc} value of 2.26 A/cm^2. Internal quantum efficiency measurements revealed outstanding short wavelength carrier collection efficiency, which is attributed to the avoidance of a growth interruption at the critical window/emitter interface that is achieved by using an $In_{0.7}Al_{0.3}As/In_{0.69}Ga_{0.31}As$ heterostructure for these lattice-mismatched MBE-grown devices. This demonstrates great promise for the use of InAlAs as an alternative window layer for InGaAs-based TPV devices.

Acknowledgement

This work was supported in part by a National Science Foundation Focused Research Group (FRG) Grant DMR-0313468.

References

[1] Hudait MK, Andre CL, Kwon O, Palmisiano MN, Ringel SA. High-performance $In_{0.53}Ga_{0.47}As$ thermophotovoltaic devices grown by solid source molecular beam epitaxy. IEEE Electron Dev Lett 2002;23(12):697–9.
[2] Hudait MK, Lin Y, Palmisiano MN, Ringel SA. 0.6-eV Band gap $In_{0.69}Ga_{0.31}As$ thermophotovoltaic devices grown on $InAs_yP_{1-y}$ step-graded buffers by molecular beam epitaxy. IEEE Electron Dev Lett 2003;24(9):538–40.
[3] Hudait MK, Lin Y, Palmisiano MN, Tivarus CA, Pelz JP, Ringel SA. Comparison of mixed anion, $InAs_yP_{1-y}$ and mixed cation, $In_xAl_{1-x}As$ metamorphic buffers grown by molecular beam epitaxy on (100) InP substrates. J Appl Phys 2004;95(8):3952–60.
[4] Coutts TJ. A review of progress in thermophotovoltaic generation of electricity. Renew Sustain Energy Rev 1999;3:77–184.
[5] Fatemi NS, Wilt DM, Hoffman Jr RW, Stan MA, Weizer VG, Jenkins PP, et al. High-performance, lattice-mismatched InGaAs/InP monolithic interconnected modules (MIMs). In: 4th NREL conference on TPV generation of electricity (AIP), vol. 460, 1999. p. 121–31.
[6] Wanlass MW, Carapella JJ, Duda A, Emery K, Gedvilas L, Moriarty T, et al. High-performance, 0.6 eV, $Ga_{0.32}In_{0.68}As/InAs_{0.32}P_{0.68}$ thermophotovoltaic converters and monolithic interconnected modules. In: 4th NREL conference on TPV generation of electricity (AIP), vol. 460, 1999. p. 132–41.
[7] Wilt DM, Murray CS, Fatemi NS, Weizer V. n/p/n tunnel junction InGaAs monolithic interconnected module (MIM). In: 4th NREL conference on TPV generation of electricity (AIP), vol. 460, 1999. p. 152–60.
[8] Yang Q, Hartmann QJ, Curtis AP, Lin C, Ahmari DA, Scott D, Kuo HC, Chen H, Stillman GE. Optimization of group V switching times for InGaP/GaAs heterostructures grown by LP-MOCVD. In: IEEE twenty-fourth international symposium on compound semiconductors. New York: IEEE; 1998. p. 95–8.
[9] Yoshioka RT, de Barros Jr LEM, Swart JW, Bettini J, de Carvalho MMG, Redolfi AG, et al. Tuning of HBT fabrication process on III–V compounds. J Solid-State Dev Circ 1999;7(1):1–6.
[10] Murray SL, Newman FD, Wilt DM, Wanlass MW, Ahrenkiel P, Messham R, et al. MOCVD growth of lattice-matched and mismatched InGaAs materials for thermophotovoltaic energy conversion. Semicond Sci Technol 2003;18:S202–8.
[11] Hudait MK, Lin Y, Goss SH, Smith P, Bradley S, Brillson LJ, et al. Evidence of interface-induced persistent photoconductivity in $InP/In_{0.53}Ga_{0.47}As/InP$ double heterostructures grown by molecular-beam epitaxy. Appl Phys Lett 2005;87:032106.
[12] Li EH. Material parameters of InGaAsP and InAlGaAs systems for use in quantum well structures at low and room temperatures. Physica E 2000;5:215–73.
[13] Wada M, Araki S, Kudo T, Umezawa T, Nakajima S, Ueda T. Temperature dependence of the band gap in $InAs_y P_{1-y}$. Appl Phys Lett 2000;76(19):2722–4.
[14] Hudait MK, Lin Y, Wilt DM, Speck JS, Tivarus CA, Heller ER, et al. High-quality $InAs_yP_{1-y}$ step-graded buffer by molecular beam epitaxy. Appl Phys Lett 2003;82(19):3212–4.
[15] Lin Y, Hudait MK, Johnston SW, Ahrenkiel RK, Ringel SA. Photoconductivity decay in metamorphic InAsP/InGaAs double heterostructures grown on $InAs_yP_{1-y}$ compositionally step-graded buffers. Appl Phys Lett 2005;86:071908.
[16] Siergiej RR, Wernsman B, Derry SA, Mahorter RG, Wehrer RJ, Link SD, et al. 20% Efficient InGaAs/InAsP thermophotovoltaic cells. In: 5th NREL conference on TPV generation of electricity (AIP), vol. 653, 2003. p. 414–23.
[17] Wernsman B, Bird T, Sheldon M, Link S, Wehrer R. Molecular beam epitaxy grown 0.6 eV n/p/n InPAs/InGaAs/InAlAs double heterostructure thermophotovoltaic devices using carbon as the p-type dopant. J Vac Sci Technol B 2006;24(3):1626–9.